European Food Research and Technology (2021) 247:1133–1148
https://doi.org/10.1007/s00217-021-03694-1

ORIGINAL PAPER

Chemical composition and microencapsulation suitability of sumac (*Rhus coriaria* L.) fruit extract

Melania Grassia[1] · Fabrizio Sarghini[2] · Maurizio Bruno[3] · Luciano Cinquanta[4] · Monica Scognamiglio[5] · Severina Pacifico[5] · Antonio Fiorentino[5] · Anna Geraci[3] · Rosario Schicchi[4] · Onofrio Corona[4]

Received: 11 October 2020 / Revised: 5 January 2021 / Accepted: 9 January 2021 / Published online: 30 January 2021

Abstract

Sumac (*Rhus coriaria* L.), a spice obtained by grinding whole sumac berries, is a complex natural product with a plethora of biological activities that can be favorably explored in nutraceutical and pharmaceutical fields. Sicilian sumac is herein chemically investigated by means of a combined NMR/HR MS-based profiling. A hydroalcoholic extract was prepared and its complexity unraveled following fractionation in an alcoholic and an aqueous fraction. The ^{1}H-NMR spectrum of this latter fraction was dominated by the signals of gallic acid and its derivatives, whereas HR MS and HR MS/MS analyses highlighted the diversity in malic acid derivatives. Gallotannins and galloyl flavonol glycosides with quercetin and myricetin as the main aglycones were highly represented in the alcoholic fraction. To improve bioavailability of chemicals in sumac extract, the feasibility of a microencapsulation process by spray drying was investigated. In particular, the addition of maltodextrin, cyclodextrin and gum arabic as covering agents was evaluated. The tests were carried out at different temperatures and concentrations. The addition of maltodextrin was found to be suitable as a carrier for the spray drying of sumac extract, having the highest yields, always > 82%. The highest values of a* (red index) and Chroma were recorded with cyclodextrin and maltodextrin at the lowest concentrations and temperatures of spray drying (120 °C). The correlations between the characteristics of the studied microcapsules (yields, moisture, total and surface polyphenols and colour) have been represented by Principal Component Analysis (PCA).

Keywords Sumac · Spray drying · Phenols · Encapsulation · Coating agent · Colour

Introduction

Last years have witnessed a considerable shift towards the choice of healthy food, devoid of chemical preservatives, because of the awareness of the possible adverse effects ascribable to synthetic antioxidants [1]. Therefore, we turned to nature as an alternative source and the addition of plant extracts as natural antioxidants to food is being increasingly explored. Meanwhile, new approaches to have a more efficient incorporation of these extracts need to be found. Several plants have been suggested as possible food additives, among these, *Rhus coriaria* L., a plant from the Anacardiaceae family. This is a shrub or small tree 1–4 m high, with imparipinnate leaves (with 9–15 leaflets). The inflorescence is a compact and erect panicle. The flowers are small, greenish-yellow colored. The fruits are 4–6 mm lenticular drupes, slightly fleshy, reddish-brown colored, surrounded by short glandular hairs, with one seed. The species, commonly known as Sumac, because the name is

✉ Luciano Cinquanta
luciano.cinquanta@gmail.com

[1] Dipartimento di Agricoltura, Ambiente e Alimenti, Università Degli Studi del Molise, Via de Sanctis, 86100 Campobasso, Italy

[2] Dipartimento di Agraria, Università Degli Studi Di Napoli Federico II, Via Università, 100, 80055 Portici, NA), Italy

[3] Dipartimento di Scienze e Tecnologie Biologiche Chimiche e Farmaceutiche, Università di Palermo, Viale delle Scienze, Ed. 17, 90128 Palermo, Italy

[4] Dipartimento Scienze Agrarie, Alimentari e Forestali, Università di Palermo Viale Delle Scienze, Ed. 4, 90128 Palermo, Italy

[5] Dipartimento di Scienze e Tecnologie Ambientali Biologiche e Farmaceutiche, Università Degli Studi Della Campania Luigi Vanvitelli, Via Vivaldi 43, 81100 Caserta, Italy

originated from 'sumaga', meaning red in Syriac language [2], is known in Italy as "Sommacco siciliano".

Rhus coriaria is a species with Mediterranean-southern distribution, cultivated up to about sixty years ago for the production of tannins and coloring substances [3]. In the Sicilian Island, it is a taxon of probable ancient introduction, as supposed by [4, 5]. Recently [6], treats this species as alien naturalized taxon among the flora of Italy, but its story would require further investigations [5]. *R. coriaria* is traditionally used as condiment, appetizer and souring agent, and the powder of its fruits is widely used as an herbal remedy thanks its anti-fibrogenic, antimicrobial, and anti-inflammatory activities [7, 8]. The hypoglycemic effect, as well as the chemopreventive efficacy of sumac were broadly investigated [9, 10]. Recently, an alcoholic extract of sumac was reported to be genoprotective, acting as a cell cycle inhibitor or apoptosis inducer [11]. Furthermore, sumac water and hydroalcoholic extracts were observed to markedly inhibit skin pro-inflammatory mediators [12]. The health promoting properties of sumac extracts are ascribable to its diversity in phenolic acids, flavonoids, and mainly to its richness in hydrolysable tannins [13–15]. These compounds are all in general known for their antioxidant properties [14]. Although the chemical composition makes sumac a good candidate as food additive, it has also been seen that polyphenols are very sensitive to heat, oxygen and light, so their concentration decreases during food processing [16–18]. Furthermore, despite their claimed health promoting properties, only a small part of them is absorbed into the gastrointestinal tract, probably because of their low solubility and permeability. Finally, when considering their use as additive, we cannot overlook the fact that they confer astringent and bitter taste to food, which makes them undesirable for most of the consumers [19, 20]. Microencapsulation technique is a way to overcome these drawbacks; it consists in the covering of a liquid, solid or gas compound (core) with a coating material (shell) [21]. In food industry, this technology is used to assure the protection of sensitive nutrients and their following controlled release [22]. Spray drying is one of the techniques used to produce a dry powder from a liquid phase in pharmaceutical and food production. The main advantage of spray drying technique is the production of stable and high-quality particles [19] with a specific size and moisture content [23]. The characteristics of the formed capsules depend on several factors that could be distinguished in operating conditions of the drying process (the inlet and outlet temperature and the flow feed), the properties of the feed (nature of coating agent and core: coating agent ratio) and structural features of the spray drier [24]. These parameters affect the particle size and morphology, their storage stability, process yield, moisture content [25] and the bioavailability of the encapsulated substances. Aware of the potential of sumac fruit as food additive, as well as of the aforementioned problems especially in terms of palatability and bioavailability of its chemical components, we propose here the microencapsulation of the polyphenol extract obtained from sumac fruits to be proposed as a method to sustain their use as food additives. Therefore, first we analyzed the chemical profile of sumac fruits grown in Southern Italy and then studied the process of microencapsulation of the extract. Three different coating agents for the encapsulation process, maltodextrin, cyclodextrin and Arabic gum were used varying the solution concentration in different concentrations and core (phenolic extract): coating material (1:1 or 1:2, v:v), two core/coating agent ratio, with different drying air temperatures. The diverse trials were evaluated by studying the capsule size, yields, moisture and phenol content (internal and superficial) of the powder product obtained from spray drying of sumac extracts.

Materials and methods

Raw material and chemicals

Sumac fruits were collected at whole ripening in three different localities in the Madonie mountains near Palermo (Sicily): Castelbuono (420 m above sea level on quartzaritic soil), Isnello (550 m above sea level on limestone rocks) and Collesano (490 m above sea level on limestone rocks). Fruits were collected in October 2018 and left to dry on a wooden shelf for about two months. They were then stored in paper bags until the time of analysis. All the samples were collected and identified by two of us (R. Schicchi and A. Geraci).

Maltodextrin (dextrose equivalent (DE) 17.0–19.9), and Arabic gum were purchased from Chimpex Industriale SPA (Caivano (NA), Italy); beta-cyclodextrin was purchased from A.C.E.F. (Fiorenzuola D'Arda (PC), Italy). Ethanol (96% v/v), methanol (99.8% v/v), acetic acid (99.8% v/v), gallic acid, calcium carbonate, Folin–Ciocalteau reagents were purchased from Sigma-Aldrich Chemical Co. (St. Louis, MO, USA). Fruits were dried at 50 °C in a ventilated oven until constant mass.

Extract preparation and chemical profile

Hydroalcoholic extract preparation

Dried and powdered plant material (50 mg) was transferred to a 2 mL microtube and mixed with 1.5 mL of phosphate buffer (Fluka Chemika, Buchs, Switzerland; 90 mM; pH 6.0) in D_2O (Cambridge Isotope Laboratories, Andover, MA, USA)—containing 0.1% w/w trimethylsilylpropionic-2,2,3,3-d_4 acid sodium salt (TMSP, Sigma–Aldrich, St. Louis, MO, USA)- and CD_3OD (Sigma–Aldrich, St. Louis,

MO, USA) (1:1). The mixture was vortexed at room temperature for 1 min, ultrasonicated (Elma Transsonic Digital, Hohentwiel, Germanys) for 40 min, and then centrifuged (Beckman Allegra™ 64R, F2402H rotor; Beckman Coulter, Fullerton, CA, USA) at 13,000 rpm for 10 min. A volume of 0.60 mL was transferred to a 5-mm NMR tube and analyzed by NMR and UHPLC-ESI-Q*q*TOF-HR MS.

Extract fractionation for chemical characterization purposes

In order to obtain partially purified fractions, an extract was prepared as described before, starting from 400 mg of dry material and using 12 mL of a MeOH:H_2O solution (1:1, v:v). The extract obtained was then purified of a C18 Sep-Pak cartridge, eluting first with MeOH and then with H_2O. The eluates were dried and analyzed by NMR and UHPLC-ESI-Q*q*TOF-HR MS.

NMR experiments

NMR spectra were recorded at 25 °C on a 300.03 MHz for ^{1}H and 75.45 MHz for ^{13}C on a Varian Mercury Plus 300 Fourier transform NMR. CD_3OD was used as the internal lock. The ^{1}H NMR was acquired with the following parameters: 0.16 Hz/point, acquisition time (AQ) = 1.0 s, relaxation delay (RD) = 1.5 s, 90°pulse width (PW) = 13.8 µs. A presaturation sequence was used to suppress the residual H_2O signal. 2D-NMR spectra were used to characterize the extracts. Standard pulse sequences and phase cycling from Varian library were used for ^{1}H, DQF-COSY, COSY, TOCSY, HSQC, H2BC, HSQCTOCSY, HMBC and CIGAR-HMBC experiments.

UHPLC-ESI-QqTOF-HR MS/MS analysis

Aqueous and alcoholic fractions from *Rhus coriaria* fruits, reconstituted in methanol LC–MS grade, at 10 mg/mL dose level, were analyzed using a Shimadzu NEXERA UHPLC system equipped with a Luna® Omega Polar C18 column (1.6 µm, 50 × 2.1 mm i.d, Phenomenex, Torrance, CA, USA). The separation of both aqueous and alcoholic fraction was achieved using a binary solution (**a**) H_2O (0.1% HCOOH), (**b**) CH_3CN (0.1% HCOOH). For analyzing the aqueous fraction, the gradient program started at 2%B and, and linearly ramped to 5%B in ten min, and to 55%B in 1 min, to then restore the initial condition, which was held for another minute. The total run time was 12 min. Alcoholic fraction was separated using a gradient program, which started at 5% B, held for 1.0 min, and linearly ramping up to 25% B in 9.50 min, and then to 55% in other 4.5 min. The solution is maintained at 55% for 5 min, and then the initial condition was restored, and held for other 2 min. The total run time was 22 min. In both the cases, the flow rate of 0.4 mL min^{-1}, and the injection volume was 2.0 µL.

MS analysis was carried out by the AB SCIEX TripleTOF®4600 (AB Sciex, Concord, ON, Canada), operating in negative ESI mode. The Q-TOF HRMS method consisted of a full scan TOF survey (dwell time 100 ms, 150–1500 Da) and eight Information Dependent Acquisition (IDA) MS/MS scans (dwell time 50 ms, 80–1300 Da). MS parameters included curtain gas (CUR) 35 psi, nebulizer gas (GS 1) 60 psi, heated gas (GS 2) 60 psi, ion spray voltage (ISVF) 4.5 kV, interface heater temperature (TEM) 600 °C. The declustering potential (DP) was set at 70 V, collision energy (CE) applied was 45 V and a collision energy spread (CES) was equal to 25 V. The instrument was controlled by Analyst® TF 1.7 software, while data processing was carried out using the PeakView® software version 2.2.

Preparation of polyphenol extract for spray drying

Polyphenols were extracted by hydroalcoholic solution [26]. The extract was then encapsulated using maltodextrin, Arabic gum and cyclodextrin as coating materials. Coating solutions (10% w/v) were prepared 1 day before the encapsulation process to obtain full dissolution in the solvent (water). For encapsulation, 1 g of lyophilized polyphenols were mixed with 1:15 and 1:30 core to coating ratio and the mixture were homogenized at 7000 rpm for 10 min using a high-speed homogenizer (DH. WHG02118, DAIHAN Scientific CO., Ltd. Korea).

Spray drying

The microencapsulation was carried by Mini Spray Dryer B-290 (Buchi Labortechnic AG, Switzerland) equipped with a nozzle two-fluid co-current. The mixture was fed at speed of 6 mL/min and the drying was performed at two different air inlet temperatures (120 and 150 °C).

Yield

The dried yield was calculated using Eq. (1)

$$Y(\%) = \left(\text{Mass of microcapsules } [g] \Big/ \text{Total mass of feed solution } [g]\right) \times 100 \quad (1)$$

Total phenolic content (TPC) and surface phenolic content (SPC)

During the spray drying process, only a part of polyphenols was entrapped in the capsules. Some of them, being a matrix system, were placed on the surface and will be lost during the following process conditions. In order to evaluate the concentration of the incorporated material (encapsulation efficiency), the polyphenols content was quantified whether on the external part of the capsules or in the whole particles by using a mixture in which they could be dissolved. The total phenolic content (TPC) was determined [27] as follow: one hundred milligrams of the prepared microcapsules were dispersed in 1 mL of an ethanol, acetic acid, and water solution (50:8:42, v:v:v). This dispersion was agitated using a Vortex (1 min) and then sonicated in an ultrasonic bath (Bandelin Electronic, Sonorex RK 100H, Germany) with 100% ultrasonic power at a frequency of 25 kHz for 20 min. The superrnatant was centrifuged at 6000 rpm for 10 min and then filtered with 0.45 µm PTFE filters (Chromacol, U.K.). The amounts of phenolic compounds were quantified by the Folin–Ciocalteau method [28]. For the determination of surface phenolic compounds (SPC), 100 mg of microcapsules were treated with 1 mL of a mixture of ethanol and methanol (1:1, v:v). These dispersions were agitated in a Vortex at room temperature for 1 min and then filtered (0.45 µm Millipore filter) [29]. The encapsulation efficiency (EE) was calculated using Eq. (2):

$$\mathrm{EE}(\%) = \left(\left[\mathrm{TPC} - \mathrm{SPC}/\mathrm{TPC}\right]\right) \times 100 \quad (2)$$

Statistical analysis

Analysis of variance (ANOVA) and Tukey's multiple range test for $p \leq 0.05$ were used to investigate the differences between all data. Principal component analysis (PCA) was applied to find the principal components contributing to most of the variance in the main physicochemical properties of samples with different coating agents. All statistical analyses were done via the SPSS Version 20.0 statistic software package (SPSS Inc., Chicago, IL, USA).

Colour properties

Colour parameters (L*, a*, b*) were measured with a CR-400 Chroma Meter (Minolta, Osaka) equipment [30]. The Hue angle H (°) and the Chroma C* values were calculated:

$$H(\circ) = \tan^{-1}(b*/a*) \quad (3)$$

$$C* = (a*2 + b*2)^{1/2} \quad (4)$$

Particle size analysis

The particle size distributions of particles were measured by a Malvern Mastersizer 3000E Hydro, (Malvern Instruments, Worcestershire, U.K.). Each different particle size measurement was done from the average of three readings per sample. Mastersizer was used by a laser obscuration greater than 10%, trials were repeated three times for each run. Results were averaged using at least 20 independent measures. The particle size was expressed as volume weighted mean diameter D [3, 4].

Results and discussion

Metabolite content of sumac extracts

Rhus coriaria has been extensively studied for its metabolites' content [8–31]. However, since the chemical composition of plant extracts can be highly variable, depending on several factors, before further proceeding with the microencapsulation a combined NMR/MS based profiling of the extract was carried out. The ^{1}H-NMR analysis of the hydroalcoholic extract showed a high complexity of the extract (Fig. 1a). Therefore, in order to have a better resolution of the signals, the extract was first partially purified on a Sep-Pack C-18 cartridge to give a water and a methanol fraction and these fractions underwent extensive 1 and 2D NMR and HR MS analysis. The NMR analysis allowed to identify the main compounds in the two fractions and, therefore, in the extract (Fig. 1).

The ^{1}H-NMR spectrum of the water fraction (Fig. 1b) was dominated by the signals of gallic and malic acids. For the first one, the only proton signal was the one detected at δ_H 7.04. However, the identity was confirmed by the 2D NMR analysis. Indeed, this signal showed HSQC correlations with the carbon at δ_C 119.9 and HMBC correlations with the carbons at δ_C 123.7, 141.2, 147.4, 170.0. These correlations are diagnostic for this metabolite and were in agreement with literature data. Furthermore, its identity is also supported by previous studies that have shown this plant to be rich in gallic acid and its derivatives [31]. Malic acid was also identified based on its 2D data that were in accordance with those previously reported [32]. Besides these two main metabolites, few other signals were detected in the aromatic region. These were in very low amount compared to gallic acid, however, COSY experiments allowed to putatively identify them as arbutin, *p*-hydroxybenzoic acid and

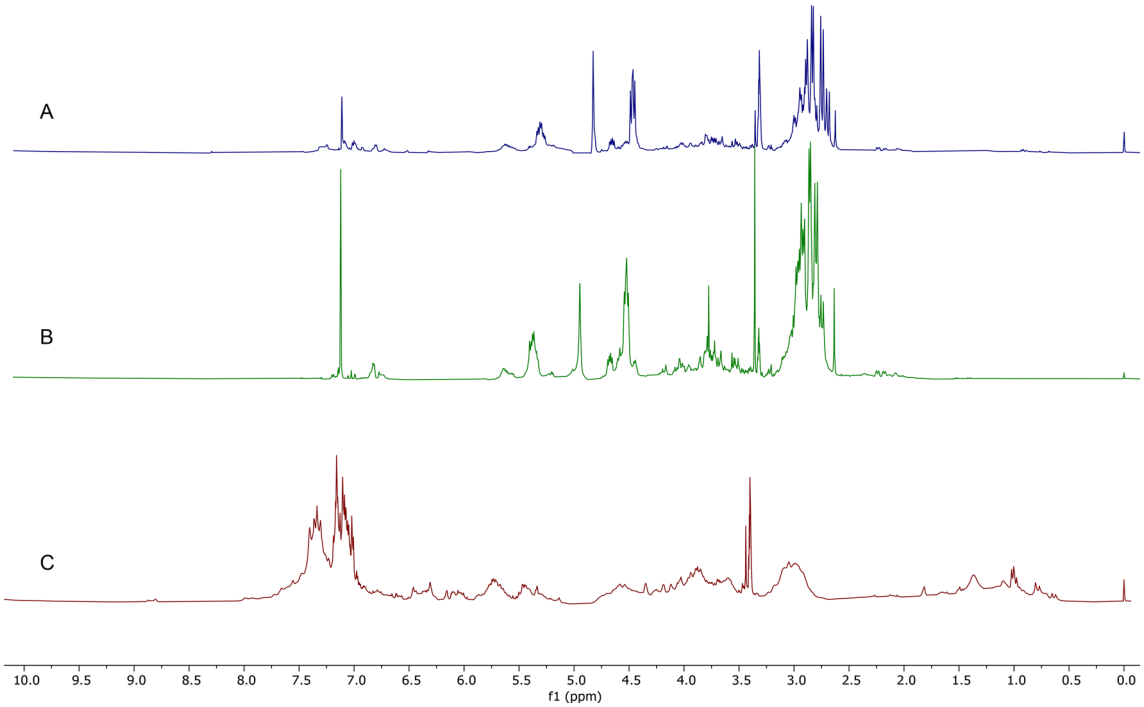

Fig. 1 ^{1}H-NMR spectra (300 MHz, MeOH-d_4: phosphate buffer in D_2O 1:1) of (**a**) *Rhus coriaria* extract; (**b**) Water fraction; (**c**) Methanol fraction

protocatechuic acid. A broad singlet observed at δ_H 6.76 was attributable to shikimic acid. This was identified thanks to the correlations observed in 2D experiments (COSY, HSQC-TOCSY, H2BC, HMBCS): these data were in agreement with those elsewhere reported [33]. Furthermore, trigonelline was identified by the singlet at δ_H 9.18, correlating in the COSY experiment with the signals at δ_H 4.45 (due to the methyl bind to nitrogen), δ_H 8.76 and δ_H 8.78. Finally, the spectrum also showed the signals of many low abundant primary metabolites.

UHPLC-ESI-Q*q*TOF-HR-MS analyses were further carried out, and twenty-four compounds were tentatively identified (Table 1). Compound 1, with the [M-H] $^-$ ion at *m/z* 191.0580, showed, beyond others, TOF-MS^2 fragment ions at *m/z* 173.0578 ([M-H-H_2O]$^-$ and 127.0404. This latter, together with the ion at *m/z* 93.0341, ensures quinic acid identity. A dimaloyl hexose was putatively compound 2, whose TOF–MS spectrum showed the deprotonated molecular ion at *m/z* 411.0791, according to the molecular formula $C_{14}H_{20}O_{14.}$ In particular, the neutral loss of a dehydrated malic acid (− 116 Da) provided the fragment ion at *m/z* 295.0637, which underwent dehydration to achieve the ion at *m/z* 277.0518 or further lost a (malic acid – H_2O) residue to give the deprotonated hexose at *m/z* 179.0522. Other maloyl glucans were compounds 4, 8, and 9, with [M-H]$^-$ ions at *m/z* 457.1198, 527.0908, and 573.1337, respectively. The TOF–MS/MS spectrum of compound 4 was in accordance with veracylglucan B, an anti-inflammatory and antiproliferative metabolite, previously isolated from aloe vera gel [34] and *Euphorbia tirucalli* [35]. In fact, the deprotonated molecular ion dehydrated to obtain the ion at *m/z* 439.1116 or was subjected to dehydrated malic acid loss for supplying the deprotonated disaccharide ion at *m/z* 341.1073. The occurrence of the compound in *Rhus coriaria* L. fruits was also reported [31], while compounds 8 and 9, which are maloyl derivatives of compounds 2 and 4, respectively, were here described for the first time. In the TOF–MS/MS spectra of both the compounds, the neutral loss of dehydrated malic acid (−116 Da), and malic acid (−134 Da) was detected. Compound 3 was malic acid. In fact, its deprotonated molecular ion at *m/z* 133.0147 provided, following the water neutral loss, the fragment ion at *m/z* 115.0040. Furthermore, di- (6), tri- (10), and tetra-malic acid (15) were also identified, whereas maloyl moiety was also a component of isocitrate (7 and 11), shikimate (12), 2-hydroxyglutarate (14), and gallate (20 and 21) depsides. Indeed, isocitric acid was recognized in compound 5, as its [M-H]$^-$ ion at *m/z* 191.0193 underwent dehydration and decarboxylation to achieve the fragment ion at *m/z* 129.0192, which further dehydrated to the ion at *m/z* 111.0091 [36]. The compound 7, which showed the [M-H]$^-$ ion at *m/z* 307.0311, was tentatively assigned, based on its TOF–MS/MS spectrum, as maloyl isocitric acid. In fact, deprotonated molecular ion lost a $C_6H_6O_6$ moiety, providing the ion at *m/z* 133.0151,

Table 1 TOF–MS and TOF–MS/MS of tentatively identified compounds in the aqueous fraction of sumac extract

Peak *n*	RT (min)	Tentative assignment	Formula	[M-H]- found (*m/z*)	[M-H]- calc. (*m/z*)	Error (ppm)	RDB	MS/MS fragment ions (*m/z*)
1	0.294	Quinic acid	$C_7H_{12}O_6$	191.0580	191.0561	9.9	2	173.0578; 127.0404; 109.0302; 93.0341; 87.0087; 85.0290
2	0.329	Dimaloyl hexose	$C_{14}H_{20}O_{14}$	411.0791	411.0780	2.6	5	411.0779; 295.0637; 277.0518; 235.0413; 205.0314; 179.0522; 161.0426; 133.0108; 115.0005; 89.0217
3	0.333	maLic acid	$C_4H_6O_5$	133.0147	133.0142	3.4	2	133.0147; 115.0040; 89.0239
4	0.343	Maloyl dihexoside	$C_{16}H_{26}O_{15}$	457.1198	457.1199	−0.2	4	457.1198; 439.1116; 341.1073; 179.0538; 161.0434; 119.0325; 89.0224
5	0.390	Isocitric acid	$C_6H_8O_7$	191.0193	191.0197	−2.2	3	191.0205; 129.0192; 111.0091; 87.0086
6	0.392	Dimalic acid	$C_8H_{10}O_9$	249.0255	249.0252	1.2	4	133.0149; 115.0040; 89.0242
7	0.426	Maloyl isocitric acid	$C_{10}H_{12}O_{11}$	307.0311	307.0307	1.4	5	133.0151; 111.0091; 87.0082
8	0.439	Trimaloyl hexose	$C_{18}H_{24}O_{18}$	527.0908	527.0890	3.4	7	527.0927; 411.0780; 393.0673; 295.0564; 277.0526; 235.0434; 205.0352; 187.0232; 179.0541; 161.0414; 133goog.0119; 115.0011; 89.0228
9	0.441	Dimaloyl dihexoside	$C_{20}H_{30}O_{19}$	573.1337	573.1309	5	6	573.1318; 457.1198; 439.1118; 341.1075; 295.0658; 241.0015; 179.0540; 161.0426; 119.0328; 89.0222
10	0.484	Trimalic acid	$C_{12}H_{14}O_{13}$	365.0364	365.0362	0.6	6	249.0265; 133.0150; 115.0040
11	0.533	Dimaloyl isocitric acid	$C_{14}H_{16}O_{15}$	423.0419	423.0416	0.6	7	289.0249; 249.0277; 191.0573; 173.0103; 133.0150; 115.0040; 111.0090
12	0.572	Dimaloyl shikimic acid	$C_{15}H_{18}O_{13}$	405.0675	405.0675	0.1	7	405.0763; 289.0600; 173.0469; 155.0361; 137.0248; 133.010; 115.0038; 93.0345
13	0.600	Gallic acid	$C_7H_6O_5$	169.0142	169.0142	−0.3	5	169.0158; 125.0252; 81.0342
14	0.608	Maloyl hydroxyglutaric acid	$C_9H_{12}O_9$	263.0409	263.409	0.2	4	147.0304; 133.0143; 129.0195; 115.0042; 87.0090
15	0.629	Tetramalic acid	$C_{16}H_{18}O_{17}$	481.0482	481.0471	2.2	8	365.0416; 347.0328; 249.0270; 133.0147; 115.0039
16	0.647	Gallic acid dimer	$C_{14}H_{12}O_{10}$	339.0353	339.0358	−1.4	9	169.0155; 125.0249
17	0.736	Digalloyl hexose	$C_{21}H_{18}O_{13}$	483.0799	483.0780	3.9	11	483.0901; 331.0733; 313.0617; 271.0499; 211.0269; 169.0161; 125.0252; 107.0142
18	1.302	Dihydroxybenzoic acid	$C_7H_6O_4$	153.0193	153.0193	−0.2	5	109.0298; 108.0219

Table 1 (continued)

Peak *n*	RT (min)	Tentative assignment	Formula	[M-H]- found (*m/z*)	[M-H]- calc. (*m/z*)	Error (ppm)	RDB	MS/MS fragment ions (*m/z*)
19	1.418	Galloyl shikimic acid i	$C_{14}H_{14}O_9$	325.0566	325.0565	0.3	8	325.0618; 169.0153; 155.0336; 125.0249; 111.0452; 93.0343
20	1.421	Maloyl gallic acid	$C_{11}H_{10}O_9$	285.0258	285.0252	2.1	7	169.0159; 133.0149; 125.0241; 115.0043; 89.0241
21	1.593	Digalloyl maloyl hexose	$C_{24}H_{24}O_{18}$	599.0923	599.0890	5.5	13	599.1062; 483.0899; 465.0768; 331.0722; 169.0157; 125.0242
22	2.050	Galloyl shikimic acid ii	$C_{14}H_{14}O_9$	325.0565	325.0565	0	8	325.0618; 173.0454; 169.0156; 125.0250; 107.0137
23	3.498	Galloyl quinic acid	$C_{14}H_{16}O_{10}$	343.0722	343.0671	15	7	343.0739; 191.0563; 169.0150; 125.0248; 107.0130
24	3.738	Digallic acid	$C_{14}H_{10}O_9$	321.0261	321.0252	2.8	10	169.0160; 125.0253

Compounds are numbered based on their RT in the whole total ion current chromatogram

RT Retention Time; *RDB* Ring Double Bond equivalent value

corresponding to malic acid, while the ion at *m/z* 111.0091 further underlined isocitric acid occurrence. The fragment ions at *m/z* 191.0573, 173.0103, and 111.0090, as well as those at *m/z* 133.0150, and 115.0040 in TOF–MS/MS spectrum of compound 11 also suggested a depside in which isocitric and malic acids are the main actors. In particular, the $[M\text{-}H]^-$ ion at *m/z* 423.0419 for compound 11 through a neutral loss of malic acid (−134 Da) provided the ion at *m/z* 289.0249, whereas the loss of isocitric acid was consistent in the ion at *m/z* 249.0277, attributable to dimalic acid. Compound 12 exhibited the $[M\text{-}H]^-$ ion at *m/z* 405.0675, which gave the ion at *m/z* 289.0600, which was likely a depside in which a hydroxy function of shikimic acid was bonded to a carboxyl group of malic acid. The deprotonated molecular ion at *m/z* 263.0409 for compound 14 was in line to a depside of malic acid and hydroxyglutaric acid. In fact, the $[M\text{-}H]^-$ ion, showed, beyond others, TOF-MS^2 fragment ions at *m/z* 147.0304, and 129.0195, which were in accordance with hydroxyglutaric acid. Finally, compounds 20 and 21 also evidenced maloyl moiety as chemical feature. Compound **20** was in line with a maloyl gallic acid as its $[M\text{-}H]^-$ ion at *m/z* 285.0258 provided through (malic acid – H_2O) neutral loss the ion at *m/z* 169.0159, due to gallic acid, which was further identified based on its decarboxylated product ion at *m/z* 125.0241. Moreover, the detection of TOF–MS/MS fragment ions at *m/z* 133.0149, and 115.0043 confirmed malic acid as a depside component. A maloyl derivative of digalloyl hexoside was tentatively compound 21, which showed its deprotonated molecular ion at *m/z* 599.0923, according to $C_{11}H_{10}O_9$ molecular formula. In fact, the neutral loss of a maloyl moiety as such (−134 Da) and as its dehydrated form (−116 Da) provided the TOF-MS^2 fragment ions at *m/z* 465.0768, and 483.0899, respectively. This latter ion was consistent with digalloyl hexose, which also was identified as constituent of this sumac fraction under peak 17. In fact, the compound **17** showed the deprotonated molecular ion at *m/z* 483.0799, which underwent in the TOF–MS/MS experiment to dehydrated gallic acid, as well as gallic acid neutral loss to achieve the fragment ions at *m/z* 331.0733, and 313.0617, respectively. The deprotonated gallic acid at *m/z* 169.0161 was detected as base peak. Thus, as highlighted by NMR spectra, gallic acid was, beyond malic acid, the other absolute actor in sumac fruits. Its presence as aglycone in glycoside derivatives, as well as in depside compounds was unraveled by TOF–MS/MS experiments, which peculiarly showed the typical loss of 152 Da, due to galloyl moiety fragmentation, and of 170 Da that corresponds precisely to gallic acid [37]. Furthermore, all the spectra of gallic acid derivatives shared deprotonated ions attributable to gallic acid and trihydroxybenzene. Compound 13 was just gallic acid, and its TOF–MS/MS spectrum showed, beyond the deprotonated molecular ion, the decarboxylation derived ion at *m/z* 125.0252. The $[M\text{-}H]^-$ ion at *m/z* 339.0353 for compound 16 was in line with gallic acid dimer, whereas the deprotonated molecular ion at *m/z* 321.0261, according to the molecular formula $C_{14}H_{10}O_9$, allowed us to putatively identify compound 24 as digallic acid, in which a depside bond was between the hydroxyl group of one gallic acid and the carboxyl group of another. Compounds 19 and 22, showing the deprotonated molecular ion at *m/z* 325.0566 and 325.0565, respectively, according to the molecular formula $C_{14}H_{14}O_9$, were assumed to be shikimoyl gallic acids. The

compound 23 was also a galloyl derivative, and it was tentatively identified, on the basis of its TOF-MS^2 spectrum, as galloyl quinic acid. Finally, deprotonated compound 18 at *m/z* 153.0193 was observed to decarboxylate producing the ion at *m/z* 109.0298, according to dihydroxybenzoic acid.

The ^{1}H-NMR spectrum of the methanol fraction (Fig. 1c) was very complex; the aromatic region, especially, was very crowded, reflecting the presence of several aromatic compounds. Among these, signals belonging to derivatives of gallic acid were detected. Unfortunately, despite the extensive 2D NMR analysis it was not possible to univocally identify these compounds. The signals of the gallic acid moieties were all in the range 7.00–7.15 ppm and showed the "classical" HMBC correlations with the carbons at δ_C 109, 139, 144, 120, 165–167. The upfield shift of the carboxyl carbons is explainable by their involvement in estereal bonds. Furthermore, the correlations of some of the latter with the signals at δ_H 5.86 (HSQC correlation with δ_C 72.8) and δ_H 5.60 (HSQC correlation with δ_C 72.9) suggested the esterification to be with sugar moieties. The presence of a spin system analogous to that of malic acid suggested the presence of this moiety esterified to other components of the extract. UHPLC-Q*q*TOF-HR-MS analysis of the alcoholic extract, of which the tentatively identified metabolites are listed in Table 2, highlighted that the most polar compound (1′) likely consisted in five maloyl moieties and one shikimoyl residue. In fact, the sequential neutral loss of -116 Da units favored fragment ions with increasing intensity that reached its maximum in the ion at *m/z* 289.0552, which tentatively corresponds to maloyl shikimic acid. The detection of the weak fragment ion at *m/z* 347.0235 suggested trimalic acid residue directly linked to dimaloyl shikimic acid core. Compound 2′ was tentatively hexamaloyl shikimic acid. Furthermore, the presence of several maloyl ester was highlighted, and promptly recognized by the characteristic neutral loss. In this context, quercetin glycosides 31′, 37′ and 42′, as well as myricetin glycuronide (19′) and glycosides (32′, and 35′). Quercetin and myricetin were the main aglycones in the highly herein represented flavonoid class. In fact, ^{1}H-NMR spectrum showed the protons of A ring resonating at δ_H/δ_C 6.17/92.5 and δ_H/δ_C 6.15/98.6, while the ring B resonances were compatible with quercetin, kaempferol and myricetin. It was reported that flavonoid derivatives including quercetin-3-*O*-rhamnoside, myricetin-3-*O*-glucoside, myricetin-3-*O*-glucuronide, and myricetin-3-*O*-rhamnoglucoside were abundant in sumac fruits [15]. In this investigation, HR-MS/MS analyses unraveled seven myricetin glycosides, whose glyconic moiety was tentatively identified based on neutral losses of 308.11 Da (17′), 162.05 Da (18′ and 26′), and 146.06 Da (24′ and 34′), as rutinose, hexose and deoxyhexose. Three myricetin glycuronides, namely 16′, 19′, and 20′, were also identified. In particular, the neutral loss of 176.03 Da, due to a dehydrated hexuronic acid, characterized the MS/MS spectra of these compounds. Compound 16′ showed the $[M-H]^-$ ion at *m/z* 493.0624, which dissociated in the TOF–MS/MS spectrum, providing the $[aglycone-H]^-$ ion as base peak. This latter at *m/z* 317.0277 showed the characteristic ions at *m/z* 299.0196, and at *m/z* 271.0246, as well as the other characteristic fragments at *m/z* 178.9994 and 151.0046 corresponded, respectively, to the retrocyclization product, and to the deprotonated A ring, released by a retro-Diels Alder mechanism. The presence of both the fragment ions at *m/z* 493.0633, and 479.0834 from the deprotonated molecular ion of compound 20′ was in accordance with myricetin hexosyl hexuronide, while, as above mentioned, TOF–MS/MS spectrum of compound 19′ suggested a maloyl hexuronide. Compounds 21′ and 30′ were also myricetin glycosides, and their tandem mass spectra were in accordance with 3,7-*O*-diglycosides [38]. The abundant ion at *m/z* 463.0882 (base peak) for compound 30′ suggested hexose moiety was linked to the hydroxyl function on C-3 carbon of the aglycone. Furthermore, compound 44′, which showed the $[M-H]^-$ ion at *m/z* 615.0992, providing after neutral loss of 152.01 Da, the ion at *m/z* 463.0863, was tentatively myricetin galloyl deoxyhexoside. Galloyl derivatives of quercetin (as such, 51′) and its deoxyhexoside derivative (50) were also identified. Overall, nine quercetin-based compounds were tentatively identified. Compounds 29′ and 39′ were monoglycosides, differing in the sugar component, whereas compounds 27′ and 28′ exhibited hexuronic acid and a disaccharide (rutinose), respectively. Compounds 36′ and 45′ were kaempferol monoglycosides. In particular, the $[M-H]^-$ ion of compound 36′ at *m/z* 447.0933, together with the ions at *m/z* 285.0376 and 284.0303 (base peak), relative to deprotonated aglycone and its radical, respectively, allowed us to identify the compound as kaempferol 3-*O*-hexoside, whereas compound 45′, which showed the $[M-H]^-$ ion at *m/z* 431.0984, and whose TOF-MS^2 experiment showed the aglycone ion as its base peak, was kaempferol 7-*O*-deoxyhexoside. Other flavonoid constituents were tentatively identified based on tandem mass spectra data in luteolin hexoside (6′) and its galloyl derivative (10′), taxifolin galloylhexoside (11′), diosmetin hexoside (12′) and catechin gallate (25′). Moreover, ellagic acid hexoside was putatively identified (14′), and its poor TOF–MS/MS spectra only showed the aglycone ion and the aglycone radical ion in remarkable intensity. The other compounds in the fraction were gallotannins, differing in galloylation degree moieties [15]. In particular, compounds 2′, 4′, 5′, 7′, and 8′, all showing the deprotonated molecular ion at *m/z* 635.089, according to the molecular formula $C_{27}H_{24}O_{18}$, were trigalloylhexose constitutional isomers. Compound 9′ was a their maloyl derivative. In fact, in TOF–MS/MS spectrum, it was observed that the ion at *m/z* 751.1000, beyond the ion at *m/z* 599.0905, attributable to the neutral loss of a (gallic acid – H_2O) residue, gave the ions at *m/z* 635.0893, due to

Table 2 TOF–MS and TOF–MS/MS of tentatively identified compounds in methanolic fraction of sumac extract

Peak n	RT (min)	Tentative assignment	Formula	[M-H]- found (*m/z*)	[M-H]- calc. (*m/z*)	Error (ppm)	RDB	MS/MS fragment ions (*m/z*)
1’	0.338	pentamaloyl shikimic acid	$C_{27}H_{30}O_{25}$	753.1009	753.1003	0.7	13	753.1156; 637.0891; 619.0788; 521.0773; 405.0664; 347.0235; 289.0552; 271.0447; 249.0243; 173.0455; 155.0348; 133.0143; 115.0036
2’	2.595	Trigalloylhexose	$C_{27}H_{24}O_{18}$	635.0890	635.0890	0	16	635.0896; 483.0771; 465.0673; 423.0559; 331.0667; 313.0556; 271.0453; 211.0453; 169.0142; 125.044
3’	3.281	hexamaloyl shikimic acid	$C_{31}H_{34}O_{29}$	869.1118	869.1113	0.6	15	869.1118; 753.1011; 637.0953; 521.0791; 503.0704; 405.0665; 289.0553; 271.0447; 249.0233; 173.0451; 133.0144; 115.0042
4’	3.394	Trigalloylhexose	$C_{27}H_{24}O_{18}$	635.0886	635.0890	0.6	16	635.0905; 483.0789; 465.0676; 423.0568; 313.0557; 295.0445; 271.0450; 211.0242; 193.0134; 169.0142; 125.0244
5’	3.429	Trigalloylhexose	$C_{27}H_{24}O_{18}$	635.0886	635.0890	0.6	16	635.0901; 483.0785; 465.0678; 423.0566; 313.0553; 295.0453; 271.0450; 211.0240; 193.0138; 169.0142; 125.0244
6’	3.807	luteolin hexoside	$C_{21}H_{20}O_{11}$	447.0933	447.0933	0	12	447.0933; 299.0537; 285.0382; 284.0305; 283.0226; 255.0277; 240.0400; 211.0375; 183.0421; 147.0064
7’	4.116	Trigalloylhexose	$C_{27}H_{24}O_{18}$	635.0891	635.0890	0.2	16	635.0893; 483.0777; 465.0672; 423.0564; 405.0457; 331.0653; 313.0554; 295.0449; 271.0450; 241.0323; 211.0242; 169.0140; 125.0246
8’	4.213	Trigalloylhexose	$C_{27}H_{24}O_{18}$	635.0891	635.0890	0.2	16	635.0892; 483.0772; 465.0665; 423.0556; 405.0449; 331.0652; 313.0553; 295.0450; 271.0450; 241.0343; 211.0241; 169.0142; 125.0244
9’	4.420	Trigalloyl maloyl hexose	$C_{31}H_{28}O_{22}$	751.0990	751.0999	-1.3	18	751.1000; 635.0893; 599.0905; 483.0782; 465.0671; 423.0562; 313.0562; 295.0451; 271.0444; 211.0241; 169.0138; 125.0247
10’	4.726	Luteolin galloylhexoside	$C_{28}H_{24}O_{15}$	599.1064	599.1042	3.6	17	599.1089; 285.0387; 257.0444; 217.0491; 125.0229

Table 2 (continued)

Peak n	RT (min)	Tentative assignment	Formula	[M-H]- found (*m/z*)	[M-H]- calc. (*m/z*)	Error (ppm)	RDB	MS/MS fragment ions (*m/z*)
11'	4.769	Taxifolin galloylhexoside	$C_{28}H_{26}O_{16}$	617.1148	617.1148	0	16	617.1154; 491.0835; 481.0987; 465.1029; 331.0662; 313.0553; 303.0502; 285.0387; 259.0606; 217.0499; 193.0137; 167.0345; 165.0189; 109.0298
12'	4.829	Diosmetin hexoside	$C_{22}H_{22}O_{11}$	461.1089	461.1089	−0.1	12	461.1089; 299.0522; 298.0458; 284.0306; 283.0217; 255.0265; 227.0329
13'	5.291	Tetragalloylhexose	$C_{34}H_{28}O_{22}$	787.0999	787.0999	−0.1	21	787.0999; 635.0877; 617.0774; 483.0745; 465.0646; 447.0537; 423.0533; 313.0524; 295.0422; 277.0312; 235.0209; 211.0211; 169.0112; 125.0216
14'	5.346	Ellagic acid hexoside	$C_{20}H_{16}O_{13}$	463.0498	463.0518	−4.4	13	463.0498; 300.9950; 299.9869
15'	5.350	Tetragalloylhexose	$C_{34}H_{28}O_{22}$	787.0999	787.0999	−0.1	21	787.1000; 635.0892; 617.0792; 483.0776; 465.0672; 447.0563; 423.0559; 313.0555; 295.0451; 277.0347; 211.0244; 169.0141; 125.0244
16'	5.824	Myricetin hexuronide	$C_{21}H_{18}O_{14}$	493.0624	493.0624	0	13	493.0626; 317.0277; 299.0196; 271.0246; 227.0316; 178.9994; 151.0046; 137.0257
17'	5.939	Myricetin rutinoside	$C_{27}H_{30}O_{17}$	625.1394	625.1410	−2.6	13	625.1406; 317.0269; 316.0201; 287.0172; 271.0224
18'	5.984	Myricetin hexoside	$C_{21}H_{20}O_{13}$	479.0834	479.0831	0.6	12	479.0835; 317.0291; 316.0222; 287.0194; 271.0245; 270.0164; 214.0268; 178.9983
19'	6.107	Myricetin maloyl hexuronide	$C_{25}H_{22}O_{18}$	609.0713	609.0733	-3.3	15	609.0735; 493.0615; 400.9799; 317.0287; 316.0192; 299.0174; 178.9989; 151.0030; 137.0236
20'	6.184	Myricetin hexosyl hexuronide	$C_{27}H_{28}O_{19}$	655.1161	655.1152	1.4	14	655.1173; 493.0633; 479.0834; 317.0299; 178.9985
21'	6.283	Myricetin dihexoside	$C_{27}H39O_{19}$	641.1366	641.1359	1.0	13	641.1352; 479.0834; 317.0291; 316.0211; 287.0165; 271.0240
22'	6.365	Tetragalloylhexose	$C_{34}H_{28}O_{22}$	787.1002	787.0999	0.3	21	787.1002; 635.0889; 617.0788; 483.0770; 465.0669; 447.0560; 423.0560; 321.0239; 313.0553; 295.0450; 277.0342; 235.0236; 211.0241; 169.0142; 125.0245

Table 2 (continued)

Peak n	RT (min)	Tentative assignment	Formula	[M-H]- found (*m/z*)	[M-H]- calc. (*m/z*)	Error (ppm)	RDB	MS/MS fragment ions (*m/z*)
23'	6.423	Tetragalloylhexose	$C_{34}H_{28}O_{22}$	787.1002	787.0999	0.3	21	787.0999; 635.0892; 617.0788; 483.0779; 465.0676; 447.0563; 429.0460; 423.0563; 313.0553; 295.0451; 277.0342; 235.0235; 211.0244; 169.0142; 125.0244
24'	6.729	Myricetin deoxyhexoside	$C_{21}H_{20}O_{12}$	463.0882	463.0882	0	12	463.0882; 317.0270; 316.0204; 287.0174; 271.0225; 214.0248; 178.9964; 151.0017; 137.0223
25'	6.888	Catechin gallate	$C_{22}H_{18}O_{10}$	441.0827	441.0827	0	14	441.0827; 289.0701; 245.0795; 203.0696; 179.0327; 137.0223; 109.0271
26'	6.891	Myricetin hexoside	$C_{21}H_{20}O_{12}$	463.0882	463.0882	0	12	463.0882; 316.0197; 301.0332; 300.0253; 271.0224; 255.0271; 243.0270; 178.9958; 151.0011
27'	6.958	Quercetin hexuronide	$C_{21}H_{18}O_{13}$	477.0675	477.0675	0.1	13	477.0675; 301.0333; 283.0232; 255.0274; 178.9962; 151.0011
28'	6.973	Quercetin rutinoside	$C_{27}H_{30}O_{16}$	609.1468	609.1461	1.1	13	609.1439; 301.0317; 300.0243; 271.0212; 255.0264
29'	7.092	Quercetin hexoside	$C_{21}H_{20}O_{12}$	463.0882	463.0882	0	12	463.0882; 301.0333; 300.0255; 271.0225; 255.0273; 243.0274; 227.0324; 178.9956; 151.0008
30'	7.168	Myricetin hexoside deoxyhexoside	$C_{27}H_{30}O_{17}$	625.1410	625.1410	0	13	625.1415; 463.0882; 317.0288; 316.0207; 271.0227
31'	7.179	quercetin maloyl hexoside	$C_{25}H_{24}O_{16}$	579.0983	579.0992	−1.5	14	579.0990; 463.0870; 300.0245; 301.0323; 271.0220; 255.0271
32'	7.469	Myricetin maloyl deoxyhexoside	$C_{25}H_{24}O_{16}$	579.0994	579.0992	0.4	14	579.0994; 463.0866; 317.0272; 316.0200; 287.0169; 271.0222
33'	7.471	Tetragalloylhexose	$C_{34}H_{28}O_{22}$	787.1002	787.0999	0.3	21	787.0999; 635.0892; 617.0788; 483.0779; 465.0676; 447.0563; 429.0460; 423.0563; 313.0553; 295.0451; 277.0342; 235.0235; 211.0244; 169.0142; 125.0244
34'	7.596	Myricetin deoxyhexoside	$C_{21}H_{20}O_{12}$	463.0891	463.0882	1.9	12	463.0882; 317.0289; 316.0211; 301.0342; 300.0261; 271.0238
35'	7.620	Myricetin maloyl deoxyhexoside	$C_{25}H_{22}O_{17}$	579.0994	579.0992	0.4	14	579.0993; 463.0881; 317.0288; 316.0216; 287.0184; 271.0235

Table 2 (continued)

Peak n	RT (min)	Tentative assignment	Formula	[M-H]- found (*m/z*)	[M-H]- calc. (*m/z*)	Error (ppm)	RDB	MS/MS fragment ions (*m/z*)
36’	7.649	Kaempferol hexoside	$C_{21}H_{20}O_{11}$	447.0933	447.0933	0	12	447.0933; 285.0376; 284.0303; 255.0273; 227.0321; 183.0417
37’	7.776	Quercetin maloyl hexuronide	$C_{25}H_{22}O_{17}$	593.0775	593.0784	− 1.7	15	593.0773; 477.0667; 301.0343; 178.9991
38’	7.900	Pentagalloylhexose	$C_{41}H_{32}O_{26}$	939.1095	939.1109	− 1.5	26	939.1109; 787.0988; 769.0878; 635.0874; 617.0765; 601.0819; 465.0640; 447.0533; 431.0583; 429.0423; 313.0519; 277.0311; 233.0417; 211.0206; 169.0107; 123.0054
39’	8.073	Quercetin deoxyhexoside	$C_{21}H_{20}O_{11}$	447.0931	447.0933	− 0.4	12	447.0933; 301.0332; 300.0254; 271.0226; 255.0277; 243.0275; 211.0378; 178.9958; 151.0016; 107.0118
40’	8.632	Pentagalloylhexose	$C_{41}H_{32}O_{26}$	939.1107	939.1109	− 0.2	26	939.1105; 787.0988; 769.0888; 635.0881; 617.0773; 601.0824; 465.0657; 447.0547; 431.0592; 429.0438; 403.0639; 313.0529; 295.0425; 233.0418; 211.0212; 169.0111
41’	8.978	Pentagalloylhexose	$C_{41}H_{32}O_{26}$	939.1116	939.1109	0.7	26	939.1109; 787.0985; 769.0884; 617.0761; 601.0809; 465.0637; 447.0532; 431.0582; 295.0412; 277.0309; 233.0408; 169.0104
42’	8.997	Quercetin maloyl deoxyhexoside	$C_{25}H_{24}O_{15}$	563.1042	563.1042	− 0.1	14	563.1042; 447.0919; 301.0323; 300.0245; 271.0214; 255.0260; 151.0006
43’	9.132	Hexagalloylhexose	$C_{48}H_{36}O_{30}$	1091.1221	1091.1219	0.2	31	1091.1219; 939.1215; 787.1206; 769.1117; 617.1095
44’	9.140	myricetin galloyldeoxyhexoside	$C_{28}H_{24}O_{16}$	615.0992	615.0992	0.1	17	615.0992; 463.0863; 317.0266; 316.0189; 271.0208; 178.9948; 151.0003
45’	9.190	kaempferol deoxyhexoside	$C_{21}H_{20}O_{10}$	431.0984	431.0984	0.1	12	431.0984; 285.0382; 284.0300; 255.0270; 227.0321; 229.0472; 183.0420
46’	9.569	Hexagalloylhexoside	$C_{48}H_{36}O_{30}$	1091.1219	1091.1219	0	31	1091.1219; 939.1101; 787.0983; 769.0877; 617.0763; 601.0819; 447.0534; 169.0106
48’	9.940	Heptagalloylhexose	$C_{55}H_{40}O_{34}$	1243.1331	1243.1328	0.2	36	1243.1327; 1091.1199; 939.1077; 787.0959; 769.0847
49’	10.152	Heptagalloylhexose	$C_{55}H_{40}O_{34}$	1243.1333	1243.1328	0.4	36	1243.1328; 1091.1195; 939.1075; 769.0861

Table 2 (continued)

Peak n	RT (min)	Tentative assignment	Formula	[M-H]- found (*m/z*)	[M-H]- calc. (*m/z*)	Error (ppm)	RDB	MS/MS fragment ions (*m/z*)
50’	10.325	Quercetin galloyl deoxyhexoside	$C_{28}H_{24}O_{15}$	599.1042	599.1042	−0.1	17	599.1042; 447.0903; 301.0320; 300.0237; 297.0578; 178.9948; 151.0002
51’	11.750	Galloyl quercetin	$C_{24}H_{14}O_{11}$	453.0463	453.0463	−0.1	16	301.0343; 178.9968; 151.0018

Compounds are numbered based on their RT in the whole total ion current chromatogram

RT Retention Time; *RDB* Ring Double Bond equivalent value

Table 3 Description of the different samples used in the microencapsulation testing of sumac extracts

Sample	Ratio*	Inlet T (°C)	Coating
M1T1	1:15	120	Maltodextrin
M1T2	1:15	150	Maltodextrin
M2T1	1:30	120	Maltodextrin
M2T2	1:30	150	Maltodextrin
C1T1	1:15	120	Cyclodextrin
C1T2	1:15	150	Cyclodextrin
C2T1	1:30	120	Cyclodextrin
C2T2	1:30	150	Cyclodextrin
G1T1	1:15	120	Arabic Gum
G1T2	1:15	150	Arabic Gum
G2T1	1:30	120	Arabic Gum
G2T2	1:30	150	Arabic Gum

*Core:coating agent ratio

Table 4 Particle size and volume distribution of the samples obtained with different coating agent (M = Maltodextrin; C = Cyclodextrin and G = Arabic Gum) at different coating ratio (1:15 and 1:30) and inlet temperatures (120 and 150 °C)

Sample	D10 (μm)	D50 (μm)	D90 (μm)
M1T1	2.34 ± 0.56^{a}	46.62 ± 3.73^{c}	142.39 ± 15.99^{a}
M1T2	11.66 ± 1.57^{c}	962.24 ± 99.91^{e}	2179.37 ± 32.35^{d}
M2T1	5.05 ± 0.29^{b}	67.84 ± 1.38^{c}	143.20 ± 5.09^{b}
M2T2	8.12 ± 0.57^{b}	69.50 ± 10.16^{c}	119.79 ± 5.62^{a}
C1T1	2.78 ± 0.53^{a}	33.20 ± 5.02^{b}	178.23 ± 13.97^{b}
C1T2	2.66 ± 0.22^{a}	65.59 ± 1.65^{c}	1301.41 ± 81.43^{d}
C2T1	1.16 ± 0.05^{a}	35.93 ± 5.05^{b}	120.86 ± 2.23^{a}
C2T2	6.27 ± 0.17^{b}	117.59 ± 8.85^{d}	2318.78 ± 28.16^{e}
G1T1	10.41 ± 1.24^{c}	66.56 ± 3.89^{c}	128.90 ± 8.91^{a}
G1T2	1.31 ± 0.10^{a}	8.43 ± 1.88^{a}	293.61 ± 37.39^{c}
G2T1	4.92 ± 0.12^{a}	56.87 ± 1.29^{c}	126.91 ± 1.92^{a}
G2T2	6.16 ± 0.64^{b}	62.87 ± 3.25^{c}	135.77 ± 1.41^{a}

Different letters within columns indicate statistically significant differences ($p < 0.05$)

the loss of dehydrated malic acid. Compounds 13′, 15′, 22′, 23′, 33′ provided the $[M\text{-}H]^-$ ion at *m/z* 787.10 and fragment ions at *m/z* 635.089 and 617.07 caused by the loss of a galloyl moiety (152 Da) and gallic acid (170 Da), respectively. Thus, these compounds were tentatively tetra-*O*-galloyl-hexoses. Analogously, compounds 40′ and 41′ were putatively assigned to penta-*O*-galloyl-hexoses, while compounds 43′ and 46′ were likely hexa-*O*-galloyl-hexoses. These latter, as well as compounds 48′ and 49′, which displayed the deprotonated molecular ion at *m/z* 1243.13 and were identified as hepta-*O*-galloyl-hexoses, did not show the neutral loss of 170 Da, confirming that galloyl moieties linked to the penta-*O*-galloyl-hexose core via a *meta*-depside bond are more cleavable than those just present on hexose nucleus.

Microcapsule size distribution

The coding of the different 12 samples (three coating agents at two concentrations and two temperatures) considered in the spray drying tests, are shown in Table 3. The first parameters studied were the particle size and the volume distribution of atomized sumac powder under different operating conditions (Table 4). The increase in inlet air temperature from 120 to 150 °C has led to an increase in the size of the particles covered by maltodextrin and cyclodextrin. Different behavior had the Arabic gums included in classes D10 (μm) and D50 (μm), the latter only at lower concentration. The increase in air drying temperature caused premature termination of the particle structure and prevented shrinkage during drying, resulting in the formation of larger particles [39]. Among the classes of particle size distribution considered, encapsulated sumac extract samples recorded the highest frequency at D90 (μm) diameter (Table 4).

Yield

The yield of sumac powder microcapsules obtained by spray drying under different process conditions was then studied. The yields varied, depending on the covering agent and process conditions (Table 5), between 85.6%

Table 5 Yield, total polyphenols (TPC) and surface polyphenols (SPC) in the different microencapsulated samples with sumac extract

Sample	Yield	TPC	SPC
M1T1	82.37	110.28 ± 1.83f	17.68 ± 1.72[b]
M1T2	83.22	84.03 ± 1.86[d]	15.42 ± 1.24[a]
M2T1	82.92	52.22 ± 0.05[b]	14.19 ± 2.69[a]
M2T2	85.57	62.15 ± 0.86[c]	15.76 ± 0.36[a]
C1T1	75.77	78.93 ± 2.32[d]	15.24 ± 1.37[a]
C1T2	78.66	84.86 ± 0.84[d]	13.71 ± 0.21[a]
C2T1	68.42	34.61 ± 1.28 [a]	15.09 ± 0.21[a]
C2T2	81.36	73.15 ± 1.69[d]	19.39 ± 0.11[b]
G1T1	73.06	123.49 ± 0.54[f]	18.86 ± 1.06[b]
G1T2	75.08	147.49 ± 2.01 [g]	14.46 ± 1.07[a]
G2T1	77.19	69.93 ± 2.29[d]	14.04 ± 0.28[a]
G2T2	65.33	64.40 ± 0.27[c]	14.41 ± 0.51[a]

Different letters within columns indicate statistically significant differences ($p < 0.05$)

(M2T2) and 65.3% (G2T2). Maltodextrins had the highest yields, always > 82%, while Arabic gum had the lowest ones. At higher temperatures and concentration (C2T2), even cyclodextrins had a high yield (81.3%). Generally, powder's yield showed an increase with the rising temperature at different core: coating material ratios. Actually, high temperature and low flow feed leads a greater efficiency in heat and mass transfer, improving the final yield [40]. The yield also rises increasing the ratio core: coating agent [41] because, in the case of maltodextrin, it reduces the deposition of particles on the wall of drying chamber [42, 43] leading to a greater trap of bioactive substances during the drying process.

Moisture content

The moisture is one of the most important to have useful information about the stability of the capsules. The highest moisture content (8.94%) was in the sample (C2T1), while the minimum content (4.64%) was in the sample with CD in (C2T2). It should be noted that this phenomenon is influenced by the greater drying rate of water evaporation at high temperature (Table 5).

Total (TPC) and surface phenol content (SPC)

The total phenol content was significantly influenced by coating agent and inlet temperature (Tab.5). The highest phenol concentrations were with Arabic gum (G1T2) (147.5 mg/100 g), followed by (G1T1) (123.5 mg/100 g) and (M1T1) (110.3 mg/100 g). Usually polyphenols are sensitive to high temperature but under the experimental conditions used, 120 or 150 °C for very short periods (about 20 s), they were not sufficient to reduce their amount. This behavior can be also explained by a higher extractability of the dried material at higher temperatures, leading to a better detection of phenolic compounds [44, 45]. These results are in accordance with those obtained by other AA [41], who studied grape polyphenols microencapsulation at different inlet temperatures. The content of surface polyphenols (SPC) was influenced by the ratio between the core and the coating agent. In fact, extreme values have been found with cyclodextrin, with a maximum SPC (19.39 g/100 g) in (C2T2) sample, and a minimum value (13.71 mg/100 g) in (C1T2).

Color

Color is an important quality factor as it reflects the sensory attractiveness and quality of powders. In fact, a functional food can provide several health benefits for consumers,

Table 6 Colour parameters (Lab values) of the samples obtained with different coating agent (M = Maltodextrin; C = Cyclodextrin and G = Arabic Gum); at different coating ratio (1:15 and 1:30) and inlet temperatures (120 and 150 °C)

Sample	*L**		*a**		*b**		hue		Chroma	
M1T1	65.58 ±	0.40[e]	14.26 ±	0.06 l	2.34 ±	0.03[f]	6.03 ±	0.06 [g]	14.45 ±	0.07[i]
M1T2	61.77 ±	0.04[a]	12.89 ±	0.02 h	2.18 ±	0.02[e]	5.86 ±	0.05[f]	13.08 ±	0.02 [g]
M2T1	65.47 ±	0.05[e]	9.12 ±	0.02 [c]	0.80 ±	0.01[a]	11.33 ±	0.11 [m]	9.16 ±	0.02[c]
M2T2	66.46 ±	0.20[f]	10.01 ±	0.02 [f]	0.29 ±	0.02[b]	7.69 ±	0.08 [l]	10.09 ±	0.02[e]
C1T1	62.34 ±	0.03[b]	13.36 ±	0.02 [i]	2.17 ±	0.02[e]	6.09 ±	0.04 [g]	13.53 ±	0.02 [h]
C1T2	62.33 ±	0.03[b]	12.86 ±	0.01 h	2.32 ±	0.02[f]	5.49 ±	0.04[e]	13.06 ±	0.00 [g]
C2T1	64.13 ±	0.01[d]	9.21 ±	0.03 [d]	1.40 ±	0.02[c]	6.51 ±	0.09 [h]	9.32 ±	0.02[d]
C2T2	67.10 ±	0.02 [g]	9.91 ±	0.02 [e]	1.44 ±	0.01[c]	6.85 ±	0.02[i]	10.01 ±	0.02[e]
G1T1	63.10 ±	0.16[c]	11.66 ±	0.02 g	2.40 ±	0.01 [g]	4.79 ±	0.01[d]	11.91 ±	0.02[f]
G1T2	61.87 ±	0.11[a]	11.60 ±	0.03 g	2.51 ±	0.04 [h]	4.55 ±	0.07[c]	11.86 ±	0.03[f]
G2T1	67.77 ±	0.01 [h]	7.54 ±	0.03 [a]	2.09 ±	0.01[d]	3.51 ±	0.03[a]	7.83 ±	0.02[a]
G2T2	63.89 ±	0.00[d]	8.29 ±	0.02[b]	2.18 ±	0.01[e]	3.72 ±	0.01[b]	8.57 ±	0.02[b]

Different letters within columns indicate statistically significant differences ($p < 0.05$)

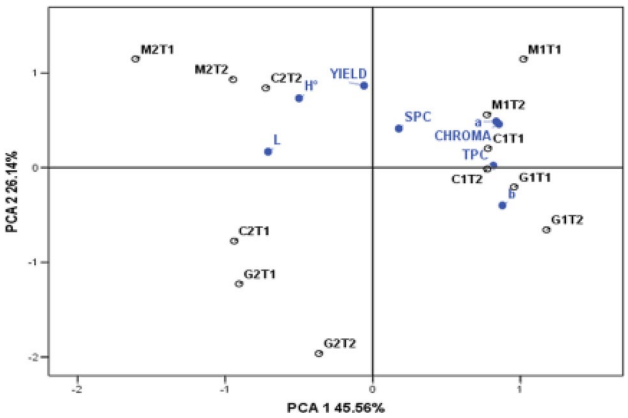

Fig. 2 Examined characteristics and samples obtained with different coating agent (M = Maltodextrin; C = Cyclodextrin and G = Arabic Gum); at different coating ratio (1:15 and 1:30; C1, G1 and G1) and inlet temperatures (120 and 150 °C; T1 and T2) in the plot of the first two principal components. *TPC* total phenol content; *SPC* superficial phenol content; L*, a*, b*, hue angle

but without visual attraction, it cannot be marketable. In general, the color values (L*, a*, b*, hue and Chroma) of the spray dried sumac extract powders were significantly influenced by the different coating agent. The highest values of a* (red index) and Chroma were recorded in C1T1 and M1T1 samples (Table 6). The decrease of these values was more accentuated by increasing the concentration of the covering agents, compared to the increase of the temperature (Table 6).

The PCA analysis

Results obtained for microcapsules properties were analyzed with the PCA method. Two main components explained 71.60% of total variation: the first one (factor 1) accounted for 45.56% and the second (factor 2) for 26.14% (Fig. 2). Samples with the lowest concentrations of maltodextrin, cyclodextrin and gum were positively correlated with the total and surface phenol content, as well as with a* and Chroma values. In contrast, the three samples with the highest concentrations of covering agents (G2T1; C2T1 and G2T2) were placed on the opposite quadrant of the above-mentioned parameters. It was also observed that the increase in maltodextrin (M2T1 and M2T2) and cyclodextrin (C2T1) content caused the results to shift to the left side of the X axis (factor 1).

Conclusion

This paper describes the characterization of a sumac hydroalcoholic extract by means of a combined NMR/MS-based profiling and the possibility to produce sumac extract microcapsules by spray drying, with the addition of different coating agents. The high chemical complexity of sumac extract was unraveled by its Sep-Pak C-18 fractionation and the obtainment of an alcoholic and an aqueous fraction. ^{1}H-NMR spectrum of the water fraction was dominated by the signals of gallic acid and its derivatives, whereas maloyl glucans and other malic acid-based compounds were detected by HR MS analysis. Gallotannins, differing in the number of galloyl moieties and galloyl flavonol glycosides were the main constituents of the alcoholic fraction. During microencapsulation process, the addition of maltodextrin was found to be suitable as a carrier for the spray drying of sumac extract, having the highest yields, always > 82%. The highest values of a* and Chroma were recorded with cyclodextrin and maltodextrin at the lowest concentrations and temperatures of spray drying (120 °C).

Compliance with ethical standards

Conflict of interest The authors declare that they have no conflict of interest.

Compliance with ethics requirements This article does not contain any studies with human or animal subjects.

References

1. Bashash M, Zamindar N (2014) Evaluation of antioxidant activities of Iranian sumac (*R. coriaria* L.) fruit and spice extracts with different solvents. J Food Meas Charact 8:213–217
2. Shabbir A (2012) *Rhus coriaria* Linn, a plant of medicinal, nutritional and industrial importance: a review. J Anim Plant Sci 22:505–512
3. Prigioniero A, Geraci A, Schicchi R, Tartaglia M, Zuzolo D, Scarano P, Marziano M, Postiglione A, Sciarrillo R, Guarino C (2020) Ethnobotany of dye plants in Southern Italy, mediterranean Basin: floristic catalog and two centuries of analysis of traditional botanical knowledge heritage. J Ethnobiol Ethnomed 16:31
4. Inzenga G (1874) Manuale pratico della coltivazione del Sommacco in Sicilia. Pedone-Lauriel, Palermo
5. Giovanelli S, Giusti G, Cionia PL, Minissale P, Ciccarelli D, Pistelli L (2017) Aroma profile and essential oil composition of *Rhus coriaria* fruits from four Sicilian sites of collection. Ind Crop Prod 97:166–174
6. Conti F, Abbate G, Alessandrini A, Blasi C (eds) (2005) An Annotated Checklist of the Italian Vascular Flora. Palombi Editori, Roma
7. Gabr SA, Alghadir AH (2019) Evaluation of the biological effects of lyophilized hydrophilic extract of *Rhus coriaria* on myeloperoxidase (MPO) activity, wound healing, and microbial infections of skin wound tissues. Evid Based Complement Alternat Med 1:5861537
8. Elagbar ZA, Shakya AK, Barhoumi LM, Al-Jaber HI (2020) Phytochemical diversity and pharmacological properties of *Rhus coriaria*. Chem Biodivers 17:e1900561
9. El Hasasna H, Athamneh K, Al Samri H, Karuvantevida N, Al Dhaheri Y, Hisaindee S, Ramadan G, Al Tamimi N, AbuQamar S, Eid A, Iratni R (2015) *Rhus coriaria* induces senescence and autophagic cell death in breast cancer cells through a mechanism involving p38 and ERK1/2 activation. Sci Rep 5:13013

10. Athamneh K, Hasasna HE, Samri HA, Attoub S, Arafat K, Benhalilou N, Rashedi AA, Dhaheri YA, AbuQamar S, Eid A, Iratni R (2017) *Rhus coriaria* increases protein ubiquitination, proteasomal degradation and triggers non-canonical Beclin-1-independent autophagy and apoptotic cell death in colon cancer cells. Sci Rep 7:11633
11. Nozza E, Melzi G, Marabini L, Marinovich M, Piazza S, Khalilpour S, Dell'Agli M, Sangiovanni E (2020) *Rhus coriaria* L fruit extract prevents UV-A-induced genotoxicity and oxidative injury in human microvascular endothelial cells. Antioxidants 9:292
12. Khalilpour S, Sangiovanni E, Piazza S, Fumagalli M, Beretta G, Dell'Agli M (2019) In vitro evidences of the traditional use of *Rhus coriaria* L fruits against skin inflammatory conditions. J Ethnopharmacol 238:111829
13. Nasar-Abbas SM, Halkman A (2003) Antimicrobial effect of water extract of sumac (*Rhus coriaria* L.) on the growth of some food borne bacteria including pathogens. Int J Food Microbiol 97:63–69
14. Kosar M, Bozan B, Temelli F, Baser KHC (2007) Antioxidant activity and phenolic composition of sumac (*Rhus coriaria* L.) extracts. Food Chem 103:952–959
15. Regazzoni L, Arlandini E, Garzon D, Santagati NA, Beretta G, Maffei Facino R (2013) A rapid profiling of gallotannins and flavonoids of the aqueous extract of *Rhus coriaria* L. by flow injection analysis with high-resolution mass spectrometry assisted with database searching. J Pharm Biomed Anal 72:202–207
16. Ross CF, Hoye C Jr, Fernandez-Plotka VC (2011) Influence of heating on the polyphenolic content and antioxidant activity of grape seed flour. J Food Sci 76:C884–C890
17. Gunathilake K, Ranaweera K, Rupasinghe H (2018) Effect of different cooking methods on polyphenols, carotenoids and antioxidant activities of selected edible leaves. Antioxidants 7:117
18. Murador D, Braga AR, Da Cunha D, De Rosso V (2018) Alterations in phenolic compound levels and antioxidant activity in response to cooking technique effects: a meta-analytic investigation. Crit Rev Food Sci Nutr 58:169–177
19. Munin A, Edwards-Lévy F (2011) Encapsulation of natural polyphenolic compounds; a review. Pharmaceutics 3:793–829
20. Cilek B, Luca A, Hasirci V, Sahin S, Sumnu G (2012) Microencapsulation of phenolic compounds extracted from sour cherry pomace: effect of formulation, ultrasonication time and core to coating ratio. Eur Food Res Technol 235:587–596
21. Gibbs BF, Kermasha S, Alli I, Mulligan CN (1999) Encapsulation in the food industry: a review. Int J Food Sci Nutr 50:213–224
22. Onwulata CI (2012) Microencapsulation and functional bioactive foods. J Food Process Pres 5:510–532
23. Keshani S, Daud WRW, Nourouzi MM, Namvar F, Ghasemi M (2015) Spray drying: an overview on wall deposition, process and modeling. J Food Eng 146:152–162
24. Handscomb CS, Kraft M, Bayly AE (2009) A new model for the drying of droplets containing suspended solids. Chem Eng Sci 64:628–637
25. Kemp IC, Hartwig T, Hamilton P, Wadley R, Bisten A (2016) Production of fine lactose particles from organic solvent in laboratory and commercial-scale spray dryers. Dry Technol 34:830–842
26. Bursal E, Köksal E (2011) Evaluation of reducing power and radical scavenging activities of water and ethanol extracts from sumac (*Rhus coriaria* L.). Food Res Int 44:2217–2221
27. Saénz C, Tapia S, Chávez J, Robert P (2009) Microencapsulation by spray drying of bioactive compounds from cactus pear (*Opuntia ficus-indica*). Food Chem 114:616–622
28. Singleton VL, Rossi JA (1965) Colorimetric of total phenolics with phosphomolybdic-phosphotungstic acid reagents. J Enol Vitic 16:144–158
29. Robert P, Gorena T, Romero N, Sepulveda E, Chavez J, Saenz C (2010) Encapsulation of polyphenols and anthocyanins from pomegranate (Punica granatum) by spray drying. Int J Food Sci 45:1386–1394
30. Alam MDR, Lyng JG, Frontuto D, Marra F, Cinquanta L (2018) Effect of pulsed electric field pretreatment on dry kinetics, color and texture of parsnip and carrot. J Food Sci 83:2159–2166
31. Abu-Reidah IM, Ali-Shtayeh MS, Jamous RM, Arráez-Román D, Segura-Carretero A (2015) HPLC-DAD-ESI-MS/MS screening of bioactive components from *Rhus coriaria* L. (Sumac) fruits. Food Chem 166:179–191
32. D'Abrosca B, Scognamiglio M, Fiumano V, Esposito A, Choi YH, Verpoorte R, Fiorentino A (2013) Plant bioassay to assess the effects of allelochemicals on the metabolome of the target species *Aegilops geniculata* by an NMR-based approach. Phytochemistry 93:27–40
33. Scognamiglio M, Schneider B (2020) Identification of potential allelochemicals from donor plants and their synergistic effects on the metabolome of *Aegilops geniculata*. Front Plant Sci 11:1046
34. Esua MF, Rauwald JW (2006) Novel bioactive maloyl glucans from aloe vera gel: isolation, structure elucidation and in vitro bioassays. Carbohydr Res 341:355–364
35. Kuster RM, Caxito MLC, Sabino KCC, da Costa HB, Tose LV, Romão W, Vaz BG, Silva AG (2015) Identification of maloyl glucans from *Euphorbia tirucalli* by ESI-(−)-FT-ICR MS analyses. Phytochem Lett 12:209–214
36. Masike K, Mhlongo MI, Mudau SP, Nobela O, Ncube EN, Tugizimana F, George MJ, Madala NE (2017) Highlighting mass spectrometric fragmentation differences and similarities between hydroxycinnamoyl-quinic acids and hydroxycinnamoyl-isocitric acids. Chem Cent J 11:29
37. Berardini N, Carle R, Schieber A (2004) Characterization of gallotannins and benzophenone derivatives from mango (*Mangifera indica* L. cv. 'Tommy Atkins') peels, pulp and kernels by high-performance liquid chromatography/electrospray ionization mass spectrometry. Rapid Commun Mass Spectr 18:2208–2216
38. Pacifico S, Piccolella S, Nocera P, Tranquillo E, Dal Poggetto F, Catauro M (2019) New insights into phenol and polyphenol composition of *Stevia rebaudiana* leaves. J Pharm Biomed Anal 163:45–57
39. Nijdam JJ, Langrish TAG (2006) The effect of surface composition on the functional properties of milk powders. J Food Eng 77:919–925
40. Tonon VR, Brabet C, Hubinger M (2011) Spray drying of acai juice: effect of inlet temperature and type of carrier agent. J Food Process Pres 5:691–700
41. Tolun A, Altintas Z, Artik N (2016) Microencapsulation of grape polyphenols using maltodextrin and gum arabic as two alternative coating materials: Development and characterization. J Biotechnol 239:23–33
42. Quek YS, Chok NK, Swedlund P (2007) The physicochemical properties of spray-dried watermelon powders. Chem Eng Process 46:386–392
43. Yang S, Mao X, Li F et al (2012) The improving effect of spray-drying encapsulation process on the bitter taste and stability of whey protein hydrolysate. Eur Food Res Technol 235:91–97
44. Kamiloglu S, Toydemir G, Boyacioglu D, Beekwilder J, Hall RD, Capanoglu E (2016) A review on the effect of drying on antioxidant potential of fruits and vegetables. Crit Rev Food Sci Nutr 56:S110–S129
45. Farina V, Cinquanta L, Vella F, Niro S, Panfili G, Metallo A, Cuccurullo G, Corona O (2020) Evolution of carotenoids, sensory profiles and volatile compounds in microwave-dried fruits of three different loquat cultivars (*Eriobotrya japonica* Lindl.). Plant Foods Hum Nutr 75:200–207